

Invited Paper

Optical Interconnects: A Solution to Very High Speed Integrated Circuits and Systems

Ray T. Chen
Physical Optics Corporation
2545 West 237th Street, Suite B
Torrance, California 90505

ABSTRACT

Microwave interference can seriously damage the performance of very high speed integrated circuits (VHSIC). The fan-out speed product is also limited by the intrinsic characteristics of electrical-interconnection. As the number of components per chip and the modulation speed increase drastically, electrical interconnection becomes inadequate on the intrachip and intrawafer levels. In this paper, optical interconnections in the intrachip, chip-to-chip, and board-to-board scenarios are investigated. A universal polymer waveguide formation method is developed. Tunability from the step index to the graded index of the polymer film provides us with the capability to construct planar and channel waveguides on any substrate including semiconductors, conductors, and insulators. A polymer waveguide modulator based on a current injection method is further developed. Modulation depth as high as 36dB has been achieved with an injection density of $1.8\mu\text{A}/\mu\text{m}^2$. The combination of the polymer microstructure passive and active devices is a powerful tool for networking active electronic devices on various architectures.

Finally, a microprism coupler ($\sim 125\mu\text{m}$) with a coupling bandwidth higher than 200nm is developed to solve the interface problems among different interconnection schemes. Using this concept, optical waves from a single-mode waveguide can be successfully coupled into a multi-mode fiber.

1. INTRODUCTION

Electromagnetic interference can seriously impair the performance of microwave integrated circuits. The problem is most serious in applications where a high degree of interconnectivity is required, such as in parallel distributed processing. In such an application, electrical interconnects exist between chips on the same circuit board as well as between circuit boards. This interference is induced by the electromagnetic interaction between waves that are generated by scattering, reflection, and resonance through the electrical wire interconnects. In addition to their susceptibility to microwave interference, metal wires and data buses are severely limited in packing density and transmission bandwidth. The last limitation is due to parasitic effects such as capacitive loading and inductive coupling in the electrical interconnects.

Optical interconnects use Bosons (photons) instead of Fermions (electrons) as the signal carrier in intrachip, chip to chip, board to board, and machine to machine communications. Due to the unique nature of Bosons, optical interconnects offer a greater fan-out speed potential and are immune to microwave interference. Optical interconnects have already demonstrated their superiority for telecommunications because of their high speed, low volume, high bandwidth, and low attenuation [1]. They also have the potential to overcome the serious electrical interconnect limitations.

Furthermore, the same optical path can route different optical signals while maintaining negligible cross talk. The combination of these outstanding features makes optical interconnects an attractive alternative for increasing the speed and parallelism and, therefore, the throughput of microelectronic systems. As the number of components per chip increases drastically, electrical interconnects become inadequate on the intrachip and intrawafer levels because they occupy a large on-chip area, which causes lower yield, reduced area for logic, and interconnect limit delays.

On the board level, the limitations of pins with electrical interconnects becomes a critical issue: Rents' rule says that the number of interconnections, U , is equal to $U^{2/3}$, where U is the number of devices^[2]. However, the minimum spacing between interconnections required by this rule happens to be about five times smaller than the minimum allowed pin spacing needed to avoid signal cross coupling in typical chips. This problem is solved by using an optical interconnect in which the minimum space between the interconnects is the size of a single-mode waveguide. Furthermore, on-chip high power sources are required to drive electrical interconnects, which is not the case for optical interconnects. Finally, unacceptable coupling between lines occurs at high speed electrical interconnects while no coupling results with optical interconnects. Because of all these considerations, optical interconnects are well suited to VLSI and ULSI intrawafer scale microwave integrated circuits and chip-to-chip communications where the problems resulting from the use of electrical interconnections are serious. This is because increasing fan-out reduces the effective impedance along the electrical interconnects and increases its propagation delay which reduces its critical line length. The density of the optical interconnects is increased since it is not affected by the signal bandwidth and since optical channels may cross in space without interaction.

In this paper, both the experimental results and further applicable optical interconnection architectures based on the fundamental building blocks, including guided wave optical devices, holographic optical elements and micropism arrays are presented. In Section 2, we introduce the major functions of guided wave optics for optical interconnects. A new polymer waveguide material, which is capable of forming guiding layer structure on any smooth surface^[3] is reported. In Section 3, holographic optical elements (HOE's) for optical interconnection are introduced. A highly multiplexed waveguide hologram is presented and experimental results are reported. Dichromated gelatin polymer grafts (DPG) were used as the holographic material for single and multiplexed grating construction. Since the index modulation of DPG holograms can be as high as 0.1^[4], a large number of gratings can be recorded on the same area of holographic emulsion. A massive fan-in and fan-out capability is provided by this technology. An active switching device is reported in section 4.0. A novel polymer waveguide modulator is designed and then tested. High extinction ratio switching device has been achieved. Finally, micropism and prism arrays are introduced in Section 5.0. Such a device is an extremely powerful tool for solving interface problems associated with many different interconnection scenarios. For example, single-mode waveguide to multi-mode fiber can be easily interconnected. Section 6.0 presents our conclusions.

2. GUIDED WAVE OPTICS

Guided wave optical elements (GWOEs), including thin film waveguides and optical fibers, are the most important building blocks for point to point optical interconnects. Unlike microwave transmission lines and guides, which may suffer serious interference due to the nature of Fermions, GWOEs are basically immune to mutual interference even if the optical paths overlap. Of course, the waveguide coupling effect needs to be eliminated by proper adjustments. Depending upon the length of the point to point interconnect, either a thin film waveguide or an optical fiber can be chosen. In this paper, the communication distance we are concerned with is relatively short (up to board to board level) so thin film waveguides are mainly employed as the optical signal carrier.

In Section 2.1, we introduce a new polymer waveguide material. It has a proven ability to form a good quality optical waveguide on any smooth surface including semiconductors, conductors, and insulators^[3]. Integration of the polymer waveguide with HOEs promises to produce a high speed, highly parallel interconnection.

2.1 Polymer Microstructure Waveguide

We report an innovative way to form low loss optical waveguides using polymer gelatin on different substrates including insulators, semiconductors and conductors. The original motivation for building gelatin waveguides was derived from the properties of dichromated gelatin (DCG). The importance of dichromated gelatin as a holographic material lies in its ability to record phase holograms by modulating the refractive

index to values exceeding 0.1^[4]. High efficiency holographic optical elements (HOEs) based on DCG have reported by various groups^[5,6]. Integration of such devices in a thin film format is very useful. However, DCG itself, due to the presence of the photosensitizer, ammonium dichromate, has serious in-plane scattering loss (>10dB/cm), which makes the formation of waveguides in conjunction with other integrated optics devices impractical.

Good quality waveguides (loss < 1 dB/cm) can be formed from pure gelatin (photo limed bone gelatin). Pure gelatin solutions with various water to gelatin ratios were spun on top of soda-lime glass (n=1.512 at 632.8nm). When the gelatin first went into an aqueous solution, upon standing at temperatures below 30°C, solutions containing more than 1% gelatin become rigid through natural cross linking and exhibited rubber-like mechanical properties. In our work, optical waveguides were thus formed. The waveguiding properties were examined by the prism coupling method. The measured effective indices for TE and TM guided waves were the same for each sample (to 0.0001 accuracy). This implies that no birefringence exists in the gelatin layer. The guiding layer index profiles of multi-mode gelatin waveguides were determined by the Inverse Wentzel-Kramers-Brillouin (IWKB) method commonly used in integrated optics ^[7,8]. The second order differential equation associated with wave propagation in a three layer dielectric waveguide is similar to the Schrodinger equation in Quantum Mechanics with N_{eff} as the eigen value, index distribution $n(x)$ as the quantum well $V(x)$, and the guided wave mode as the wave function^[9]. The WKB approximation reduces the solution of the eigenvalue problem, boundary conditions at the guide surface, to the solution of the equation

$$\int_0^{dn} \left[N^2(x) - N_{eff_n}^2 \right]^{1/2} dx = \frac{4n-1}{8} \quad n = 1, 2, \dots \quad (1)$$

where dn is defined by $N(dn) = N_{eff_n}$. We also let $d_0 = 0$ and $N_{eff_0} = N_0$. This treatment is good because the effective index of the 0th order mode of a waveguide with many modes is very close to the surface index. The graded index profile of a multi-mode waveguide can be accurately determined by the IWKB method. Step indices can be also determined through this method with a small deviation at the turning point^[10]. The calculated index profile of sample #D1, composed of 15 grams of gelatin (photo limed bone gelatin), 100cc water, and spun at 100rpm, is given in Figure 1, Curve A. The depth of the step index profile is equal to the film thickness.

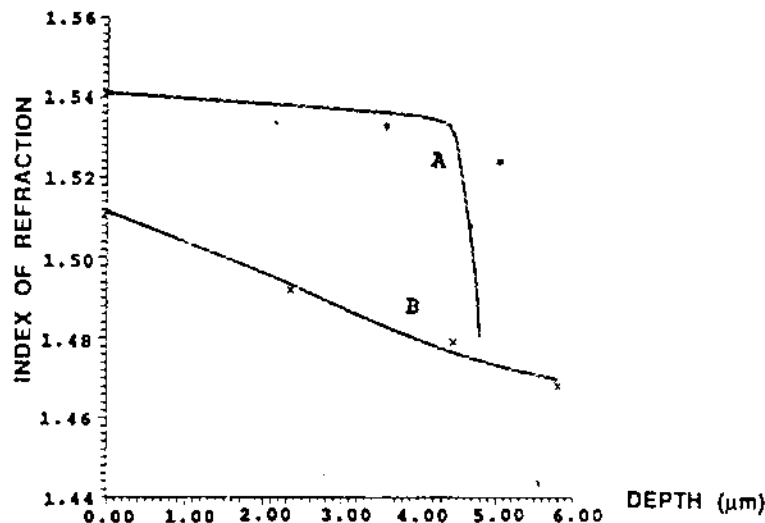


Figure 1. Index Profile of Gelatin Waveguide D1. Curve A, Before Wet Processing; Curve B, After Wet Processing.

The measured surface refractive index of various samples with index variation from 1.522 to 1.543 was observed. Each data point of Figure 2 was determined by the 0th order mode effective index. The plotted index profiles of the various gelatin waveguides before wet processing, a method associated with DCG hologram fabrication^[11], demonstrate that the gelatin layer forms a step index layer and the index of refraction increases as the gelatin ratio increases.

Wet processing, associated with DCG hologram fabrication, followed immediately after the above experiment. The gelatin layer was made to swell in water, and then was dehydrated with isopropyl alcohol^[11]. The waveguide parameters were measured again. Propagation loss less than 1 dB/cm was observed on various substrates. The waveguide loss remained low (<1dB/cm) after wet processing. The index profiles were shifted to a graded index

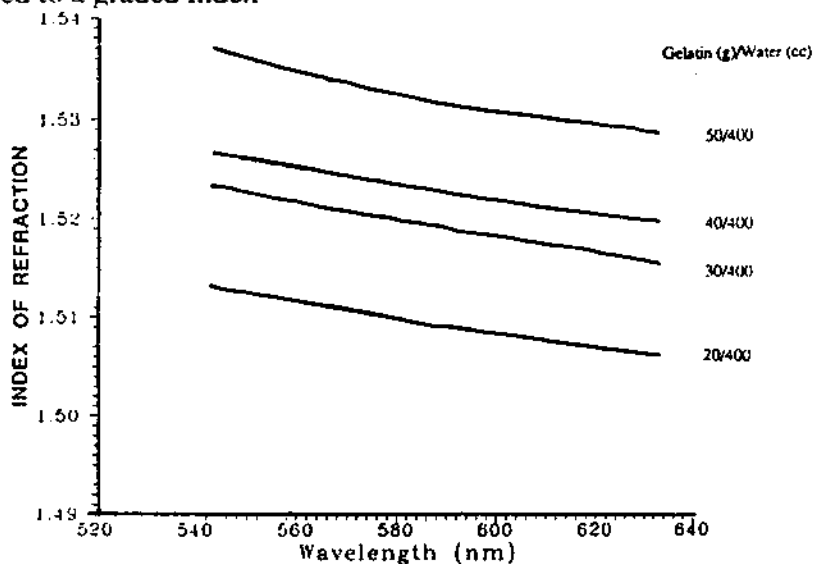


Figure 2. Refractive Indices of Gelatin Layer at 632.8 nm as a Function of Gelatin Weight in 100 cm³ of Water Solution before Wet Processing.

with a lower surface index than the initial film. Profiles ranging from approximately linear to approximately Gaussian can be produced by choosing different wet processing procedures. The result for sample #D1 after wet processing is shown in Figure 1, Curve B. The same tendency, i.e. a decrease of the surface index and a change of the index profile from a step index to a graded index distribution, has been consistently observed on all samples measured. This index distribution is similar to a graded index fiber. The lower index portion of the gelatin layer functions as a cladding layer for the formation of the waveguide. The basic material used for waveguide fabrication has extreme temperature stability. The initial results indicate that the optical parameters, such as transparency and optical density, will remain unaffected even if the temperature variation ranges from -180°C (liquid nitrogen) to 160°C for several hours and 200°C for tens of minutes^[12].

The results described above imply that waveguides with mode indices lower than the substrate index can be constructed. For example, sample #D1 has three modes with mode indices lower than the substrate index 1.512 (Figure 1). With an index profile like this, waveguide structures can be formed on any smooth surface regardless of its index of refraction and conductivity. We have spun gelatin layers on PC board, and GaAs and Al₂O₃ substrates. Photographs of waveguiding in graded index waveguides made by this process are displayed in Figures 3 (a) to (d), corresponding to glass, PC board, and GaAs and Al₂O₃ substrates respectively. Graded index profiles after wet processing have also been confirmed on PC board, and GaAs and Al₂O₃ substrates. The index profiles determined by IWKB on these substrates are similar to glass. The general shape of the gelatin layer after wet processing is shown in Figure 4. Profiles ranging from approximately linear to approximately Gaussian can be produced by choosing different wet processing procedures.

2.2 Formation of Channel Waveguide

The index of refraction tuning method provides us with an easy and cost-effective way to generate a planar waveguide structure suitable for any substrate. However, to further make this type of device useful to coplanar interconnection, there are two major technical issues that need to be addressed. First, the real estate of wafer surface has to be effectively employed. High packing density of VLSI chips allows us to have a very limited area applicable to point to point interconnection. Second, the signal carriers, photons in this case, can be routed in a non-colinear manner, i.e., to transmit optical signals in a curved structure. The feasible solution to solve these two problems simultaneously is to generate a channel waveguide. A negative rib channel waveguide is designed that is shown in Figure 5. The polymer microstructure waveguide is coated with $d_1 < d_{\text{cutoff}} < d_2$ which allows only the rib region to have the waveguiding property. Similar to the polymer planar waveguide formation on a high index

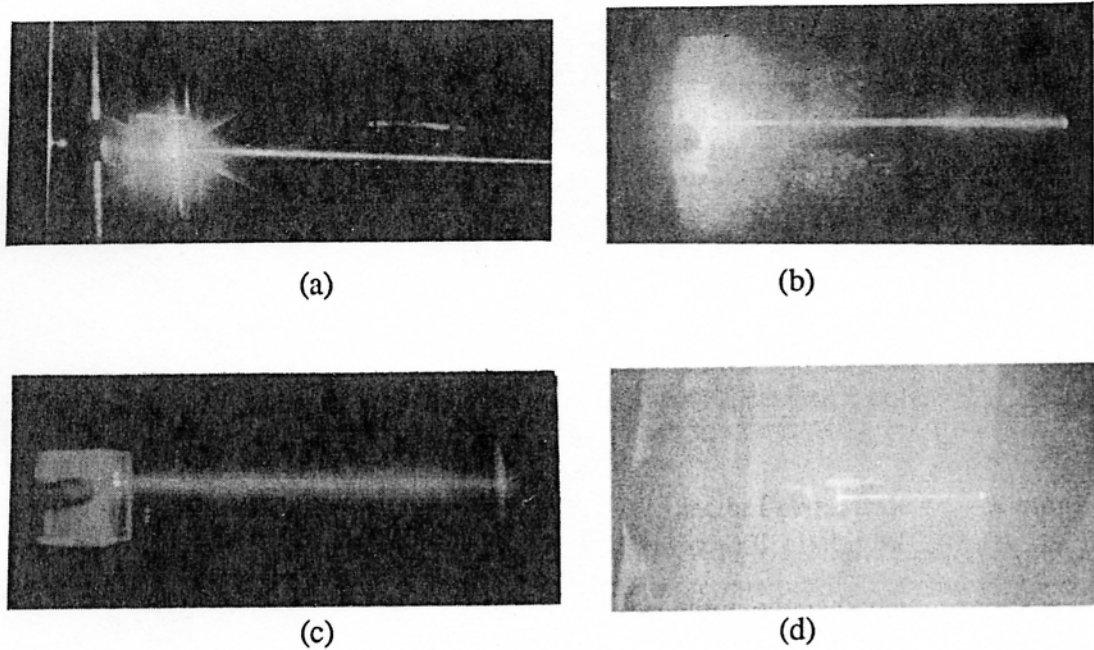


Figure 3. Polymer Microstructure Waveguide on (a) Glass, (b) PC Board, (c) GaAs and (d) Al_2O_3 .

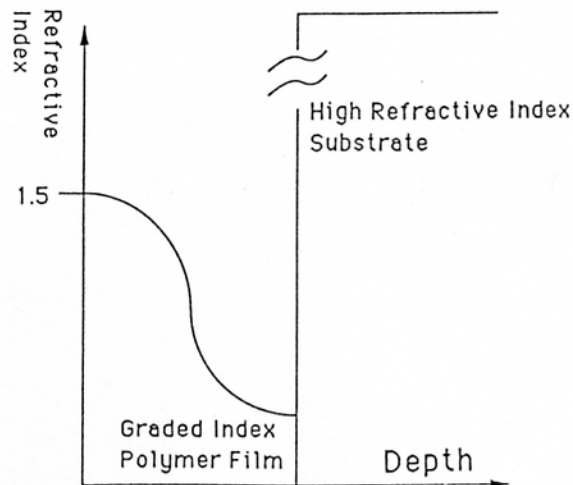


Figure 4. General Shape of the Polymer Gelatin Film After Wet Processing.

substrate [3], the index tuning method is employed to construct two dimensional graded index profile which provides us with channel waveguiding capability regardless of the refractive index and the conductivity of substrate materials. Refractive index profile tuning due to the wet process results in a graded index profile for both horizontal and vertical directions.

The experimental result on a silicon substrate is shown in Figure 6. Negative rib waveguide bends, curves, branches, and intersections can be made by using conventional microlithography in conjunction with an etching process. A multimode channel waveguide array with losses ranging from 3 to 5 dB/cm is observed. More efforts are needed to reduce the propagation loss. It is to be noted that the communication distance of intrawafer and interchip is relatively short and therefore, the multi-mode channel waveguide design shall give us a less stringent

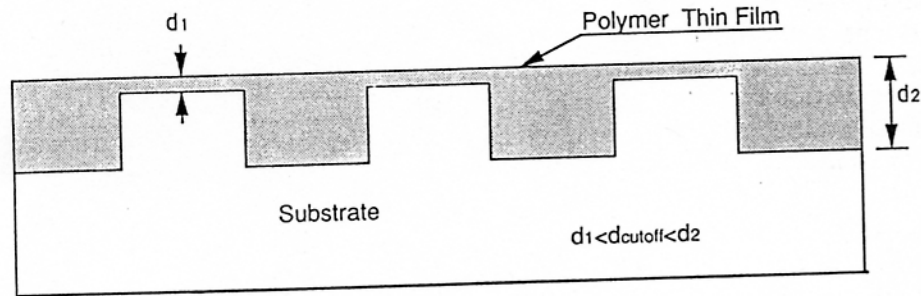


Figure 5. Negative Rib Channel Waveguide (Side View).

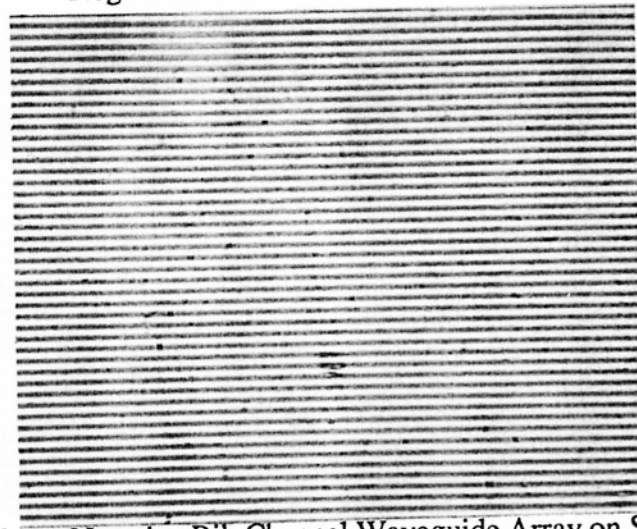


Figure 6. 10 μm Negative Rib Channel Waveguide Array on Si Substrate.

power budget and better tolerance of environmental instability such as temperature and humidity. The basic requirement for optically implementing intrawafer, chip-to-chip, board-to-board, and backplane optical interconnections is to construct a process compatible, optical network linking the active network interface sites. The tunability of the guiding layer index of the polymer gelatin provides us with a universal method to construct a high quality channel and planar waveguides on any thin film substrate. Such compatibility opens a new avenue to perform high speed interconnection on both hybrid and monolithic optoelectronic systems.

Optical interconnects on Microwave Integrated Circuits, using a thin film waveguide, represent a far reaching effort to apply thin-film technology to optical circuits and devices and to develop better and more

economical optical systems. One of the major building blocks required to fulfill the above scheme is a good quality optical waveguide that can receive and propagate optical signals with minimum loss and yet be integrated with various passive and active devices on different substrates. The difficulty in building such good quality optical waveguides on various electro-optic crystals is one of the major reasons that high speed opto-electronic devices are fabricated primarily on LiNbO₃ and III-V heterostructures (GaAs-GaAlAs, InP-GaInAsP, etc.). For example, SBN has an electro-optic coefficient r₃₃ more than one order of magnitude higher than that of LiNbO₃. However, the tremendous propagation losses of SBN:60 waveguides^[13] make it impractical to build any passive or active devices on this substrate. Materials that can be placed on different electro-optic substrates, form good quality waveguides, and be integrated with other optoelectronic devices are necessary to solve this problem. The waveguide material we introduce here gives us a new method to construct an optical waveguide on various optoelectronic substrates to route optical signals. The feasibility of making a polymer waveguide modulator, which will be discussed in Section 4.0, based on the same waveguide material, allows us to build a reconfigurable interconnection network.

Construction of good quality optical microstructure planar and channel waveguides, based on the polymer gelatin thin film, opens a wide range of plausible applications. Due to the limitation of conventional integrated circuits, such as fan-out capability, modulation speed, electromigration and electromagnetic interference, interconnections and signal processing using photons are widely agreed as a promising alternative for next generation communication systems. The polymer microstructure waveguides we report herein provide us with a new method to access optical interconnection, signal processing, and computing on various scenarios.

3. WAVEGUIDE HOLOGRAM

Holographic Optical Elements (HOEs) have been reported previously^[15-19] as a means for optical interconnects. Herein, a novel guided wave HOE for intraplane massive fanout interconnection is presented. Multiplexed waveguide holograms need to be implemented to provide one-to-many fan-out and many-to-one fan-in. High efficiency waveguide hologram can be constructed by locally sensitizing the polymer thin film with ammonium dichromate. A grating coupler that converts free space TEM₀₀ laser light to a two-dimensional spherical guided wave with a 50° angle of divergence was demonstrated. Figure 7(a) is a side view of the device; Figure 7(b) is a photograph of the waveguide coupling. An optical clock distribution network and a passive broadcasting network are feasible with this new technology. Moreover, the availability of high index modulation of the sensitized film and the large interaction length of the waveguide geometry allow us to implement a highly multiplexed hologram in the same locally sensitized area. If a grating in the one-to-many interconnection architecture has a similar Δn value, the maximum number of gratings that can be implemented in the same waveguide hologram is estimated to be ^[14]

$$N = \frac{2 \cdot \Delta n_{\max} d \varphi}{\lambda \cos \theta} \quad (2)$$

where Δn_{max} is the maximum achievable index modulation of the DCG material, θ is the Bragg diffraction angle, d is the interaction length and 0 < φ ≤ 1 depending on the polarization of optical wave and the diffraction angle. For example, a transverse magnetic (TM) guided wave with λ=500nm, φ=1 and d=500μm and θ=45°, we have N=282 fan-outs/rad.

In the real time implementation, the upper limit of grating multiplexing is governed by either the power budget or the cross-talk induced signal to noise ratio which is correlated with the in-plane scattering and the base bandwidth of the optical carriers. The results shown in this paper and other publications^[14,19] have the highest fanout number reported thus far.

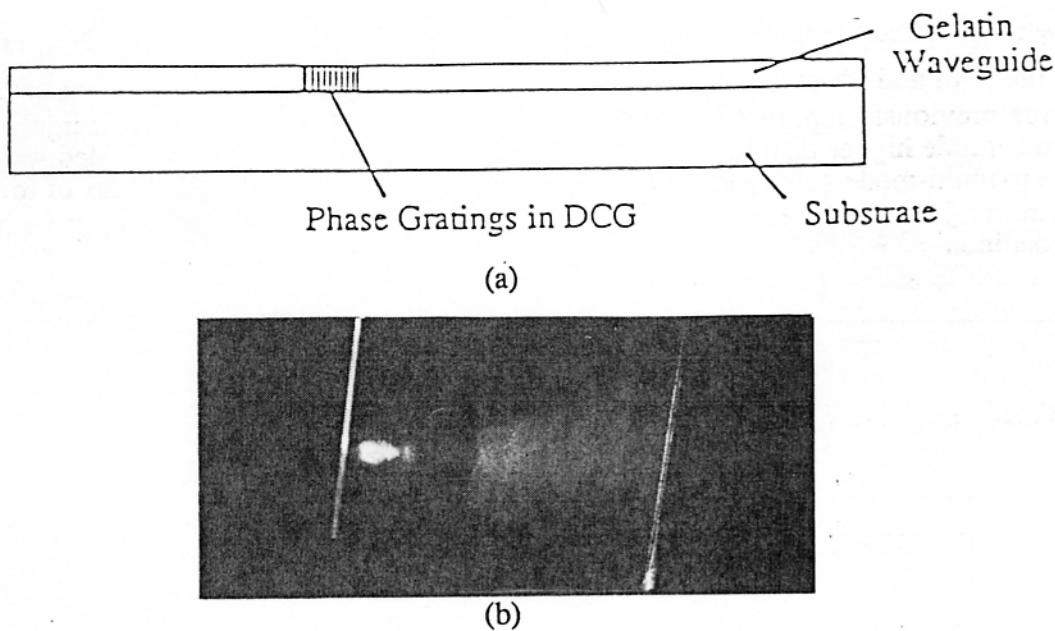


Figure 7. Coupling of 488nm TEM₀₀ Free-Space Laser Radiation into a Two-Dimensional Spherical Wave with a 50° Beam Divergence in a Gelatin Waveguide. (a) Cross Section of the Device, (b) Real Photograph of the Grating Coupler.

4. POLYMER WAVEGUIDE MODULATOR

We report, for the first time, a novel collinear electro-optic modulator on a polymer microstructure waveguide which can be on any smooth surface including semiconductors, conductors and insulators. A single-mode collinear modulator was made, based on the heterowaveguide structure shown in Figure 8. The substrate can be any thin film of interest; for example, GaAs, LiNbO₃, Al₂O₃, Si, etc. The first layer is a waveguide with multiple modes. Formation of the waveguide was carried out by tuning the index such that the substrate index does not influence waveguiding on the low index polymer film. The second layer is a transparent semiconductor film In_{1-x}Sn_xO_y ($n=1.74$ at $\lambda=632.8\text{nm}$) whose index of refraction can be modulated by current injection. The In_{1-x}Sn_xO_y film is thinner than the cut off thickness supporting a fundamental mode. Finally, a single-mode polymer waveguide is coated and tuned on top of the semiconductor film. The schematic of the refractive indices of the multilayer are shown in Figure 8(b) and the measured effective indices of two heterostructure waveguides are shown in Figure 9. The effective indices of the multimode guide were measured right after the conducting film formed. There are a total of 10 modes on the first guide.

Explanation of the mechanism of modulation now follows. The first polymer multi-mode waveguide was made thick enough to support a large number of guided mode. The second single-mode polymer waveguide was made such that the mode index is within the numerical value of the effective indices of the multiple mode waveguide, i.e.,

$$N_{m_{i-1}} < N_{\text{eff}} < N_{m_i} \quad (3)$$

where N_{eff} is the effective index of the single-mode waveguide and $N_{m_{i-1}}$ and N_{m_i} are the effective indices of the $(i-1)$ th and i th modes, respectively. The change of the refractive index caused by current injection was previously reported [20]. The index modulation generated by current injection can be two orders of magnitude higher than linear electro-optic effect. Transferring of the guided wave from single-mode guide to multi-mode guide and vice versa was fulfilled by shifting the film index of $\text{In}_{1-x}\text{Sn}_x\text{O}_y$ (ITO) through current injection. An electrical current is injected into the semiconductor layer such that the phase matching condition

$$N_{\text{eff}} = N_{m_i} \quad (4)$$

can be achieved. It is to be noted that the coupling constant K for dual channels is defined by [21]:

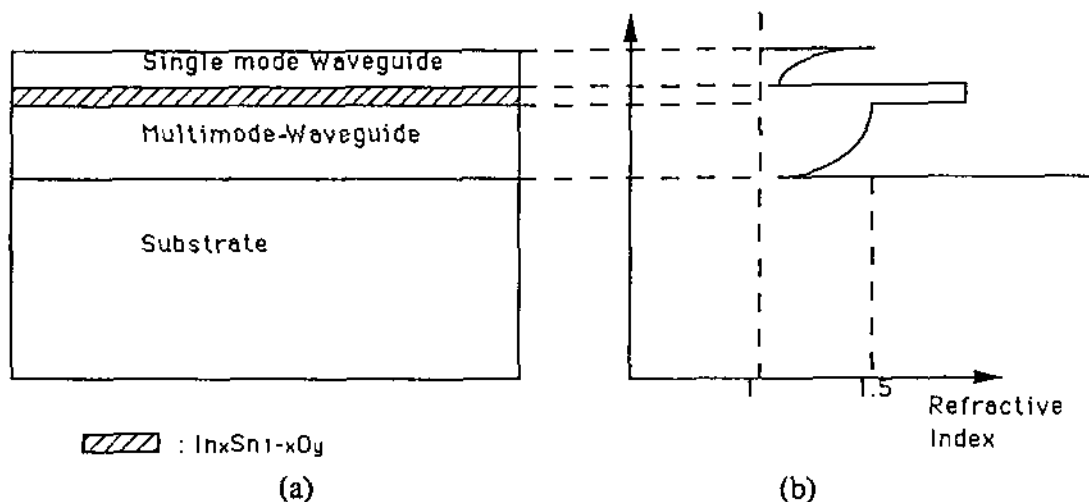


Figure 8. (a) Device Structure of Single-Mode Polymer Waveguide Modulator
(b) Schematic of the Refractive Index Distribution of Heterostructure Multilayer

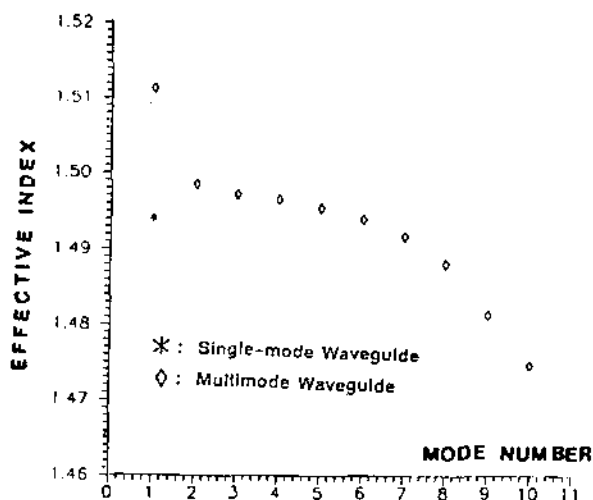


Figure 9. Effective Indices of Two Colinear Waveguides Associated with Device Structure Shown in Figure 8.

$$K = \left\langle \psi_s \left| \frac{i\omega\Delta\epsilon(x,y)}{4} \right| \psi_{m_i} \right\rangle \quad (5)$$

where ω is the angular frequency of the optical wave, $\Delta\epsilon(x,y)$ is the difference of the dielectric coefficients between the waveguide and the cladding layers, and ψ_s and ψ_{m_i} are the mode profiles of the single-mode and the i th mode of the multi-mode waveguide, respectively. Deviation from the criterion set by Eq. (4) will automatically generate a mismatch phase term in Eq. (5) which, depending upon the quantity of mismatch, may result in a zero coupling coefficient. Actually, this is the situation without an external perturbation. It is clear from Figure 8 that the maximum index modulation needed to generate the phase matching condition is

$$\Delta n = (N_{m_{i-1}} - N_{m_i}) \quad (6)$$

Note that the index modulation within the $\text{In}_x\text{Sn}_{1-x}\text{O}_y$ film mainly changes the effective indices of the multi-mode waveguide (Figure 8(b)). Equation 6 explains the reason for the requirement of a highly multiple mode waveguide. To reduce the current injection and therefore, the microwave power consumption, the mode separation of the multi-mode waveguide also needs to be controlled.

The device structure made for the feasibility demonstration is illustrated in Figure 10. The demonstration was made on a glass substrate. The current is injected into the ITO film through the ohmic contact and the optical wave is coupled into the single-mode waveguide through a prism coupler. The throughput intensity is monitored by a vidicon camera. Since the polymer waveguide can be constructed on any smooth surface, the multilayer structure can be implemented on any material of interest. The experimental result under different current densities was performed. The intensity of the single-mode m-dot as a function of applied current with 1 cm interaction length is shown in Figure 11. Index modulation due to current injection is independent of the polarization of guided waves. Modulation depth as high as 36dB was observed with current density of $1.8\mu\text{A}/\mu\text{m}^2$.

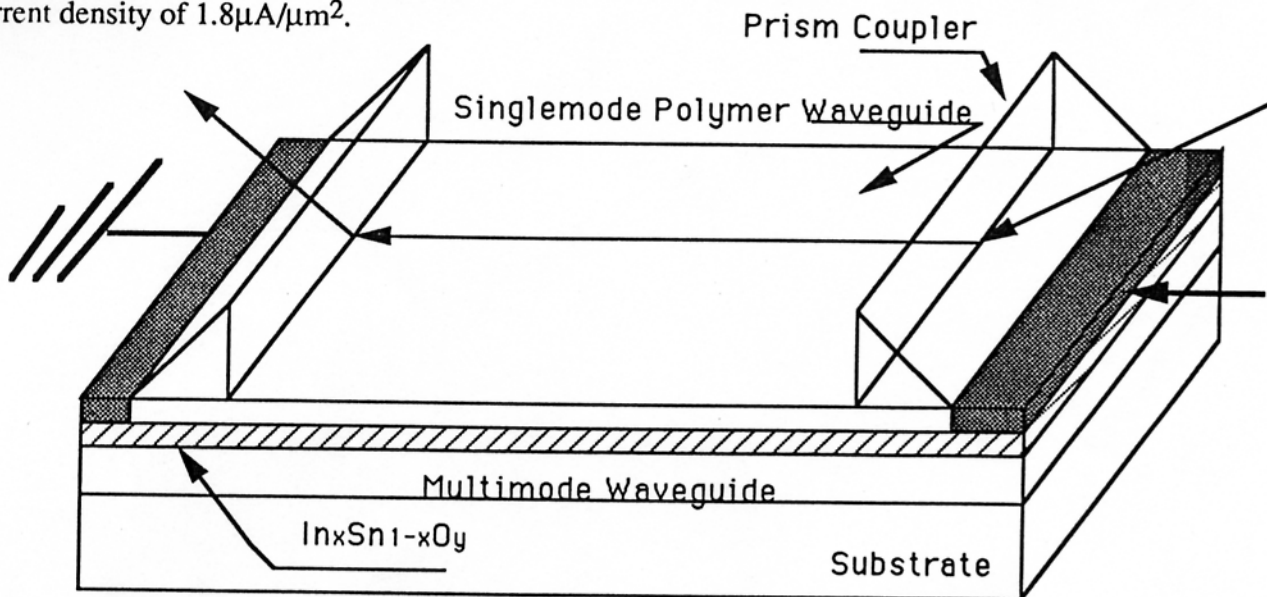


Figure 10. Device Structure for Feasibility Demonstration.

The electrode structure shown in Figure 10 is similar to a travelling wave electro-optic modulator^[22]. Accordingly, the modulation bandwidth Δf shall be governed by

$$\Delta f = \frac{2V_c V_o}{\pi(V_o - V_c)L} \quad (7)$$

where V_c and V_o are the phase velocity of current and optical waves, respectively, and L is the interaction length. Note that the cutoff frequency is determined by the walk-off speed between the optical wave and the injected current. Equation 7 is valid if the recombination time of the minority carriers and other time dependent modulation mechanisms are faster than the switching speed.

The polymer waveguide material and the ITO conducting film show an excellent transparent bandwidth from 300nm to 2800nm over which a series of useful wavelengths for optical communication is located. As a result, a large number of applications can be realized using the proposed architecture. Furthermore, the polymer waveguide material has been proven to be capable of forming high quality planar and channel waveguides on any smooth surface, including semiconductor, conductors, and insulators regardless of its conductivity and index of refraction. Local area network, CATV, optical sensors, optical signal processing and computing, and coherent communication are some of the most useful scenarios where the polymer waveguide modulator can be an attractive device.

5. MICROPRISM ARRAY FOR WIDE BAND COUPLING

The aforementioned experimental results provide us with an easy and universal means to construct passive and active devices for optical communication and signal processing. However, interfaces between discrete devices are the major bottle necks for realizing a large interconnection network. For example, there is no efficient way to couple a guided wave from a single mode waveguide to a multi-mode fiber. A waveguide coupler made out of a

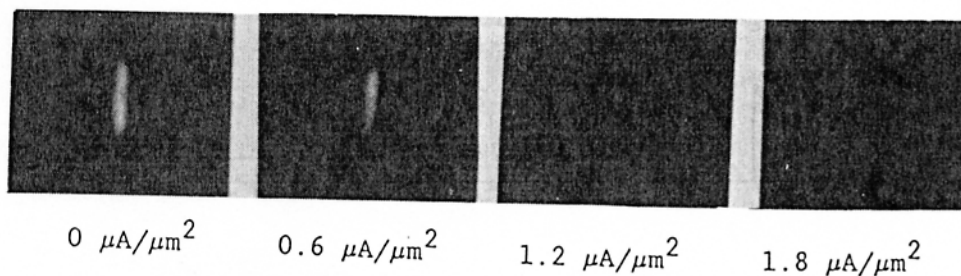


Figure 11. Intensity Modulation Under a Different Current Injection.

holographic grating is intrinsically narrow band due to the fixed grating spacing and the phase matching condition. We have demonstrated a 200nm wide band prism coupling device. The extraordinarily large bandwidth is due to the same tendency of waveguide and prism dispersion as the function of optical wavelength. The well-known phase matching condition for prism coupling is:

$$N_{\text{eff}} = N_p \cos \left(\sin^{-1} \left(\frac{\sin \alpha}{N_p} \right) \right) \quad (8)$$

where N_{eff} is the effective index of the waveguide mode, N_p is the index of the prism, and α is the incident angle of laser beam. When the optical wavelength becomes shorter, the same trend of decline of N_p and N_{eff} allows us to efficiently couple an optical wave into a single waveguide from 632.8nm to 830nm while keeping α as a constant.

Although prism coupling can provide us with much wider coupling bandwidths, the conventional prism coupler still can not efficiently couple light from waveguide to fiber. The in-plane scattering and Gaussian beam divergence enlarge the prism-coupled spot size (either m-dot or m-line) in the direction perpendicular to the guided wave propagating direction. The larger the prism, the larger the spot size. The diameter of the spot coupled out from a single-mode waveguide by using a micro prism is compatible with multi-mode fibers (50/125, 62.5/125, 100/140 μm). The spot size out of the conventional prism is too large to be matchable. Again, to date, there is no practical way to couple optical waves from single-mode integrated optical devices to multi-mode fibers. The innovative method we developed provides an easy and feasible way to solve this interface problem.

Recently, several microprism series have been developed at POC. Their applications are continuously being explored. The extremely small size of the prisms yield new applications in fiber optics, integrated optics, and micro-optics.

Microprism fabrication falls into two categories: (1) direct drawing, i.e., a fiber is pulled into a prism shape, and (2) plate cutting, which allows the microprism to be any shape. The prism side dimensions range from $\sim 0.1\text{mm}$ to 3mm . Dimension tolerance can be controlled within a few microns. The materials used can be glass, fused silica, crystal, and fused optical materials. Figure 12 shows a photograph of a microprism ($\sim 125\ \mu\text{m}$ in size) as a waveguide coupling device^[23].

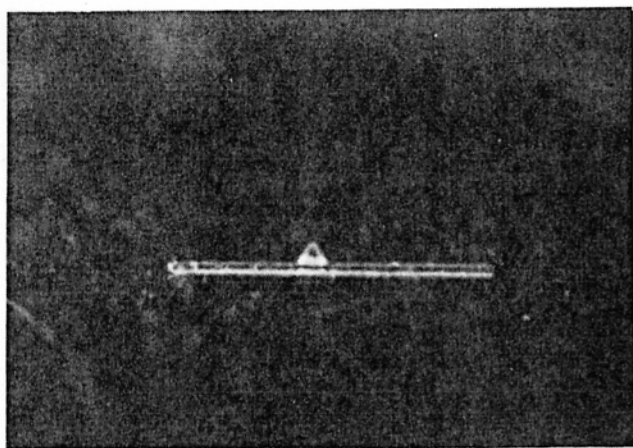


Figure 12. Microprism ($\sim 125\ \mu\text{m}$) as a Wide Band Waveguide Coupler.

6. CONCLUSION

In summary, man made noise, such as electromagnetic interference (EMI) and electromagnetic pulse (EMP) can seriously damage the performance of very high speed integrated circuits (VHSIC). As the packing density and speed requirement become more stringent, optical interconnection is a very attractive alternative. Due to the intrinsic characteristic of photons, massive fan-out networks with a larger base bandwidth, which is not achievable through electrical interconnection, have proven to be feasible using optical interconnection.

In this paper, a universal polymer planar and channel waveguide, and a polymer waveguide modulator are developed. Such devices can be implemented on any substrate of interest regardless of its refractive index and conductivity. The refractive index tuning method provides us with a graded index (GRIN) distribution which facilitates the formation of both planar and channel waveguides on any surface. Further integration of polymer waveguide passive and active devices with micropism and prism arrays furnishes us with a wide band coupler suitable for many scenarios of optical interconnections. For example, coupling from single-mode waveguide to multi-mode fiber can be successfully made out of this device.

The basic requirement for optically implementing intrawafer, chip-to-chip, board-to-board and backplane optical interconnections is to construct a process compatible optical network linking the active network interface sites. The tunability of the guiding layer index of the polymer gelatin provides us with a universal method to construct a high quality channel and planar waveguides on any thin film substrate. Such compatibility opens a new avenue to perform high speed interconnection on both hybrid and monolithic optoelectronic systems.

7. ACKNOWLEDGEMENT

The participation and contribution by Michael R. Wang, Lev Sadovnik, Huey Lu, Daniel Robinson, Olga Demichovskaia, and Zonjian Sun in the various research projects described in this paper are gratefully acknowledged. Helpful discussions with Drs Tomasz Jansson and Joanna Jansson are also acknowledged. Formation of highly multiplexed waveguide hologram for VLSI optical interconnection is supported by SDI (Contract No.DASG 60-89-C-0053 and DASG60-90-0018) and the development of the polymer gelatin waveguide modulator is supported by NSF (Contract No. NSF89-61123).

8. REFERENCES

1. J.E. Midwinter, "Current Status of Optical Communication Technology," *J of Light Wave Technology*, Vol. LT-3, 927 (1985).
2. J.W. Goodman, F.J. Leonberger, S.Y. Kung and R.A. Athale, "Optical Interconnections for VLSI Systems," *Proceedings of IEEE*, Vol. 72, pp. 850-865 (1984).
3. R.T. Chen, W. Phillips, T. Jansson and D. Pelka, "Integration of Holographic Optical Elements with Polymer Gelatin Waveguides on GaAs LiNbO₃, Glass and Aluminum," *Optics Letters*, August 15 (1989).
4. T. Jansson and J. Jansson, "High Efficiency Bragg Holograms in the IR, Visible UV and XUV Spectral Region," *SPIE Vol. 883*, pp. 84-93 (1988).
5. B.J. Chang and C.D. Leonard, "Dichromated Gelatin for the Fabrication of Holographic Optical Elements," Vol. 14, p. 2407 (1979).
6. S.S. Duncan, J.A. McQuoid and D.T. McCartnet, "Holographic Filter in DCG Position Tuned Over the Near Infrared Region," *Optical Engineering*, "Vol. 24, pp. 781-785 (1985).
7. C. Schiff, *Quantum Mechanics* (Mc Graw-Hill) New York, pp. 267-280 (1975).
8. P.K. Tien, R. Ulrich and R.J. Martin, "Modes of Propagating Sight Waves in Thin Deposited Semiconductor Films," *Applied Physics Letters*, Vol. 14, pp. 291-293 (1969).
9. R.T. Chen and W.S.C. Chang, "Anomalous Attenuation on Y-cut Proton Exchanged LiNbO₃ Waveguides," *IEEE J. Quantum Electron*, QE-22-880-882 (1988).
10. J.M. White and P.F. Heidrich, "Optical Waveguide Refractive Index Profile Determined from Measurement of Mode Indices, A Simple Analysis," *Applied Optics*, Vol. 15, pp. 151-155 (1976).
11. D. Meyerhofer, "Holographic Recording Materials," Chap. 3, Vol. 20, *Topics in Applied Physics*, Springer-Verlag (1977).
12. T. Jansson, G. Savant, and Y. Qiao, "Holographic Rugate Structures for X-ray Optics Applications", Annual Report, FG03-86ER13600, Department of Energy.
13. O. Eknoyan, C.H. Bulmer, H.F. Taylor, W.K. Burns, A.S. Greenblatt, L.A. Beach and R.R. Neurgaonkar, "Vapor Diffused Optical Waveguides in Stratum Barium Niobate," *Applied Physics Letters*, Vol. 48, pp. 13-15 (1988).

14. R.T. Chen, Michael R. Wang and Tomasz Jansson, "Intra-plane Guided Wave Massive Fanout Optical Interconnects," Accepted for publication in Applied Physics Letters (1990).
15. Davis H. Hartman, "Digital High Speed Interconnects - a Study of the Optical Alternative," Optical Engineering, Vol. 25, pp. 1087-1102 (1986).
16. Bradley D. Clymer and Joseph W. Goodman, "Optical Clock Distribute to Silicon Chips," Optical Engineering, Vol. 25, p. 1103-1108 (1986).
17. L.A. Bergman, W.H. Wu, A.R. Johnston, R. Nixon, Sadik C. Esener, C.C. Guest, P. Yu, Timothy J. Drabik, M. Feldman and Sing H. Lee, "Holographic Optical Interconnects for VLSI," Optical Engineering, Vol. 25, 1109-1118 (1986).
18. W. Driemeier, "Bragg-effect Grating Couplers Integrated in Multicomponent Polymeric Waveguides," Optics Letters, Vol. 15, pp. 725-727 (1990).
19. Michael R. Wang, Ray T. Chen, Greg J. Sonek and Tomasz Jansson, "Wavelength-Division Multiplexing and Demultiplexing on Locally Sensitized Single-Mode Polymer Microstructure Waveguides," Optics Letters, Vol. 15, pp. 363-305 (1990).
20. A. F. Evans and D. G. Hall, "Measurements of the Electrically Induced Refractive Index Change in Silicon for 1300nm Wavelength using a Schottky Diode," Appl. Phys. Lett., Vol.56, 212-215(1990) and R. Soref and J.P. Lorenzo, "All Silicon Active and Passive Guided-Wave Components for $\lambda=1.3$ and $1.6 \mu\text{m}$," IEEE J. Quantum Electron, Vol. QE-22, pp. 873-879 (1986).
21. Ray T. Chen, "Polymer Gelatin Waveguide Modulator," Final Report to National Science Foundation, Contract No.NSF89-61123.
22. Rod C. Alferness, "Guided-Wave Devices for Optical Communication," IEEE J. Quantum Electron, Vol. QE-17, pp. 946-959 (1981).
23. Zonjian Sun, Internal Report of Physical Optics Corporation 1990 and "Smallest Prism Made in NIST," United States Department of Commerce News, p. 30 (April 17, 1990).